



Efficacy of Octacalcium Phosphate/Gelatin (OCP/Gel) Composite Implantation for Miniature Swine Lumbar Interbody Fusion

Yu Mori,¹ Ryo Hamai,² Ryuichi Kanabuchi,¹ Takahiro Onoki,¹ Kohei Takahashi,¹
Ko Hashimoto,¹ Toshimi Aizawa¹ and Osamu Suzuki²

¹Department of Orthopaedic Surgery, Tohoku University Graduate School of Medicine, Sendai, Miyagi, Japan

²Division of Craniofacial Function Engineering, Tohoku University Graduate School of Dentistry, Sendai, Miyagi, Japan

Synthetic octacalcium phosphate (OCP) has emerged as a potential precursor for bone apatite crystals, promoting faster bone formation and better biodegradability compared to hydroxyapatite and β -tricalcium phosphate materials. Combining OCP with various polymeric biomaterials enhances its ductility, making it suitable for clinical applications, including dentistry. Preclinical studies on OCP/gelatin (OCP/Gel) composites have shown excellent osteoconductive and osteoinductive properties, indicating potential for bone defect repairs. This study investigates the efficacy of OCP/Gel as a filler for lumbar interbody fusion cages. A miniature swine model underwent surgery using polyetheretherketone (PEEK) cages with different fillers: no filler, autologous rib, and OCP/Gel. Eight weeks post-surgery evaluations using computed tomography, histological assessments, and Fourier transform infrared (FT-IR) spectroscopy revealed that while PEEK cages without fillers showed no bone fusion, those with autologous rib and OCP/Gel demonstrated partial interbody fusion. Histological analysis indicated new bone growth in cages with OCP/Gel, and FT-IR spectroscopy confirmed the degradation of OCP at the vertebral interface and increased bone matrix proteins. The findings suggest that OCP/Gel could be a viable alternative to autologous bone grafts for lumbar interbody fusion surgeries, offering less invasive and more cost-effective solutions. The success of OCP/Gel in clinical applications could pave the way for broader use in orthopedic reconstructive surgeries, potentially eliminating the need for combined use of bone marrow aspirate or expensive growth factors.

Keywords: bone graft substitute; gelatin; interbody fusion; octacalcium phosphate; osteogenesis

Tohoku J. Exp. Med., 2025 June, 266 (2), 135-144.

doi: 10.1620/tjem.2024.J138

Introduction

In recent years, advances in the understanding of the mechanisms of bone induction and improvements in bone graft substitutes have made synthetic bone an attractive alternative to autologous bone grafting (Tamai et al. 2002; Ogose et al. 2006; Suzuki et al. 2006). Currently, available bone graft substitute options include β -tricalcium phosphate (β -TCP) (Bohner et al. 2020) and a porous hydroxyapatite/collagen composite (HA/Col) made from nanoscale HA and type I collagen from pigs (Kikuchi et al. 2001). Animal models and clinical trials have shown good biodegradability,

high osteoconductivity, and bone regeneration ability when used to treat defects in long bones (Ogose et al. 2005; Sotome et al. 2016). In particular, the elastic material properties of HA/Col are an important characteristic of this bone graft substitute when used as an interbody fusion cage filler, as they reduce the risk of the cage falling out when inserted into the intervertebral disc space (Sotome et al. 2016).

On the other hand, while most bone graft substitute materials have been proven to be both biocompatible and osteoconductive, few cases have shown osteoinductive properties (LeGeros 2002; Giannoudis et al. 2005). Therefore, there are high expectations for developing materials with

Received August 11, 2024; revised and accepted November 13, 2024; J-STAGE Advance online publication November 28, 2024

Correspondence: Yu Mori, Department of Orthopaedic Surgery, Tohoku University Graduate School of Medicine, 1-1 Seiryomachi, Aoba-ku, Sendai, Miyagi 980-8574, Japan.

e-mail: yu.mori.c4@tohoku.ac.jp

Osamu Suzuki, Division of Craniofacial Function Engineering, Tohoku University Graduate School of Dentistry, 4-1 Seiryomachi, Aoba-ku, Sendai, Miyagi 980-8575, Japan.

e-mail: suzuki-o@tohoku.ac.jp

©2025 Tohoku University Medical Press. This is an open-access article distributed under the terms of the Creative Commons Attribution-NonCommercial-NoDerivatives 4.0 International License (CC-BY-NC-ND 4.0). Anyone may download, reuse, copy, reprint, or distribute the article without modifications or adaptations for non-profit purposes if they cite the original authors and source properly.

<https://creativecommons.org/licenses/by-nc-nd/4.0/>

biologically active bone-inducing properties.

Octacalcium phosphate (OCP) has been proposed as a precursor of bone apatite crystals (Brown 1966). Previous studies have shown that (1) synthetic OCP induces faster bone formation than HA materials and is more biodegradable than β -TCP, but when implanted in various intramembranous and long bone defect animal models, its structure is converted to Ca-deficient HA (Imaizumi et al. 2006; Kikawa et al. 2009; Miyatake et al. 2009; Murakami et al. 2010; Sato et al. 2019), (2) OCP promotes osteoblast differentiation and osteoclast formation *in vitro*, while its structure is converted to a bone apatite crystal-like Ca-deficient HA (Suzuki et al. 2006; Anada et al. 2008; Takami et al. 2009; Hamai et al. 2022), (3) combining OCP with various synthetic and natural polymeric biomaterials improves the ductility of OCP as an alternative material (Handa et al. 2012; Ezoe et al. 2015; Chiba et al. 2016; Ishiko-Uzuka et al. 2017; Baba et al. 2020; Kawai et al. 2020; Oizumi et al. 2021; Hamada et al. 2022). The OCP/collagen complex has undergone clinical trials in dentistry and is now available for clinical practice (Kawai et al. 2020). Preclinical studies have also reported that OCP/gelatin (OCP/Gel) composites have excellent osteoconductive and osteoinductive properties with a better-handling property that can be used to repair bone defects even in a transcortical defect, and their future clinical application is expected (Grecula 2022; Mori et al. 2023). Regarding the handling property, a previous mechanical testing study has shown that OCP/Gel composite can be repeatedly deformed under cyclic compressive strain loading conditions where OCP/Gel composites were immersed in culture media (Yamada et al. 2015).

There have been reports on the usefulness of HA/Col bone graft substitutes as filling materials for posterior lumbar interbody fusion cages. However, there is still room for further investigation into the usefulness of these interbody fusion cage-filling materials (Kushioka et al. 2018; Yoshii et al. 2021). On the other hand, the advantage of OCP/Gel is that they are expected to promote interfacial activity and bone formation due to their excellent conformity to the vertebral endplate. Therefore, OCP/Gel may be more suitable as filling materials for lumbar interbody fusion cages. This study aims to clarify the usefulness of the OCP/Gel composite as a filling material for cages used in lumbar interbody fusion by examining its osteoinductive and osteoconductive properties in detail in a miniature swine lumbar interbody fusion model.

Materials and Methods

Preparation of OCP/Gel composite

A residue of OCP has been synthesized using the wet synthesis method, as described in a previous report (Suzuki et al. 1991). In brief, OCP was prepared using a wet synthesis method, mixing calcium and phosphate solutions at 65°C to 70°C. During mixing, the degree of supersaturation concerning OCP and HA in the preparation solution was set in the range of 4×10^{11} and 1×10^{18} , respectively,

whose values were calculated at 25°C (Honda et al. 2007). The precipitated OCP was separated and washed. The synthetic OCP was subsequently dried and sieved to obtain granules with particle sizes ranging from 50 μ m to 250 μ m. The OCP/Gel composites were prepared according to the method previously reported (Hamada et al. 2022). In brief, 77% by weight of the total weight of OCP was homogenized with the gel solution at 4°C for 24 hours. The OCP/Gel composite was frozen at -20°C for 24 hours and lyophilized for 72 hours to form a porous structure. The thermal cross-linking treatment of the OCP/Gel composites was carried out under a vacuum at 150°C for 24 hours. OCP/gel composite material was molded into a 1.5 mm thick plate and cut to fit inside the cage.

Animals and Surgical procedure

A female Clawn miniature swine was used for the experiment. A miniature swine weighing 20 kg was obtained from CLEA Japan (Tokyo, Japan). An anterior lumbar interbody fusion was performed between three vertebrae. After the surgery, the miniature swine was not restricted in its behavior. All animal procedures and husbandry were conducted in accordance with the rules established by the Association for Assessment and Accreditation of Laboratory Animal Care (AAALAC), and all experiments were managed and supervised with the permission of the Tohoku University School of Medicine Animal Experiment Committee (Protocol No: 2021MdA-107-01). The miniature swine received a pre-surgical sedation consisting of a muscle injection of xylazine (2.0 mg/kg) and butorphanol (0.2 mg/kg). After the sedation, the animal was intubated and then underwent surgery under general anesthesia with Isoflurane (2.0%). Cephalosporin (1.0 g, intravenously) was administered as a prophylactic antibiotic 30 minutes before surgery.

The miniature swine was secured in the lateral decubitus position before surgery, and the target level was confirmed using fluoroscopic images. A skin incision of approximately 25 cm was made from above the 15th rib to the anterior aspect of the L6 vertebra. At the stage where the external and internal oblique muscles were developed in the abdomen, the 15th rib was developed and harvested for subsequent bone grafting. The transverse abdominal muscle was divided bluntly, the transverse abdominal fascia was dissected posteriorly to create an extraperitoneal space, and the psoas muscle was exposed. Disc resection was performed at lumbar 2/3 (L2/3), L3/4, and L4/5, and a polyetheretherketone (PEEK) cage was inserted into the disc space. The PEEK cage was fabricated from commercially available medical grade PEEK material (PEEK-OPTIMA Natural, Invibio, West Conshohocken, PA, USA) that can be inserted into the lumbar intervertebral disc space of miniature swine. The cage size was 9 mm in width, 20 mm in length, and 4 mm or 5 mm in thickness, as appropriate. A cage alone was inserted into the disc space at L2/3, a cage with an autologous rib was inserted into the disc space at

L3/4, and a cage with OCP/Gel was inserted into the disc space at L4/5. After cage insertion, the abdominal muscles and rectus sheath were carefully sutured, and the skin closed. Prophylactic cephalosporin (1.0 g, intravenously) was administered for 1 day postoperatively. All miniature swine were housed in individual cages and fed a normal diet.

Computed tomography evaluation

A 16-row multi-slice computed tomography scanner (Supria, Hitachi, Tokyo, Japan) was used 8 weeks after surgery to observe the changes over time in the miniature swine's lumbar interbody fusion. Computerized 3D reconstruction was performed using 3D analysis software (OsiriX MD, Bernex, Switzerland), as a previous report (Kogure et al. 2019).

Non-demineralized histological assessment

Non-calcified sections were prepared to histologically detect the interbody fusion effect between the PEEK cage alone, the PEEK cage and autologous ribs, and the PEEK cage and OCP/Gel-treated vertebral bodies. The lumbar vertebrae of the miniature swine were cut in the middle of the vertebrae so that the samples could be evaluated individually for each of the L2/3, L3/4, and L4/5 intervertebral discs. According to the reported procedure, non-calcified tissue sections were prepared for histological analysis (Tanaka et al. 2016; Ito et al. 2022; Koguchi et al. 2023). To explain briefly, the collected implant tissue was immediately immersed in a 70% ethanol solution and fixed for 5 days. The samples were stained with Villanueva bone staining for 6 days. The tissue was dehydrated in ethanol in stages and degreased in a solution of acetone/methyl methacrylate monomer (1:3). The degreased tissue was embedded in methyl methacrylate. The vertebral bodies were cut along the coronal plane to produce tissue sections 200 μm thick. To obtain sections 40 μm thick, the tissue on the slide was polished using a precision lapping machine (Maruto Instruments, Tokyo, Japan). Images of the cross sections were taken using a slide scanner (VS200, Olympus, Tokyo, Japan).

Fourier Transform Infrared (FT-IR) spectroscopy assessment

The relative distribution of protein and calcium phosphate was evaluated using infrared imaging to investigate the osteogenic effects of OCP/Gel samples implanted in the vertebrae of miniature swine. Analysis was carried out using a Hyperion 3000 FT-IR microscope (Bruker Japan, Yokohama, Japan). After the surface was polished and adjusted, analysis was carried out on samples in which PEEK cages and OCP/Gel were implanted into the L4/5 intervertebral disc space. The measurement conditions were as follows: pixel size of 1 $\mu\text{m}/\text{pixel}$, resolution of 4 cm^{-1} , measurement wavelength range of 2,000 to 750 cm^{-1} , number of integrations of 64, and measurement area of 288 $\mu\text{m} \times 288 \mu\text{m}$. The evaluation was conducted on the forma-

tion of calcium phosphate and bone matrix protein, which reflected the contact between the cage and the vertebrae in the L4/5 intervertebral disc space and the bone formation in the center of the cage using OCP/Gel.

Results

Computed tomography

Computed tomography images taken 8 weeks after interbody fusion surgery showed no evidence of bone fusion with the PEEK cage without bone graft or bone graft substitute. However, the combination of the PEEK cage and autologous rib graft showed evidence of partial interbody fusion, and the combination of the PEEK cage and OCP/Gel also showed evidence of partial interbody fusion (Fig. 1).

Non-demineralized histological assessment

No signs of interbody fusion were observed in the PEEK cage without bone graft or bone graft substitute, and only fibrous tissue growth was observed. In interbody fusion using autologous ribs and a PEEK cage, new bone was observed in the intervertebral disc space in addition to the autologous ribs. In interbody fusion using an OCP/Gel and a PEEK cage, vigorous new bone was observed from the contact surface of the vertebrae to the margins of the PEEK cage and OCP/Gel placed in the intervertebral disc space. Furthermore, findings inside the PEEK cage suggested bone formation, and the OCP granules were resorbed and irregular in size. OCP/Gel may induce bone formation inside the PEEK cage (Fig. 2).

FT-IR spectroscopy assessment

Fig. 3 shows the image measurement results of the central part of the PEEK cage implanted with OCP/Gel. The relative distribution is visualized by mapping the absorption intensity ratio divided between the amide I and phosphate groups. The accumulation area of the phosphate group, indicating OCP particles, is large, while the accumulation area of the amide I group, suggesting bone matrix-derived proteins, is small.

Fig. 4 shows the IR spectra extracted from the arrowed points (black, green, and red arrows) in the imaging measurement results in Fig. 3. Peaks mainly derived from acrylic embedding resin (indicated in the Figure), amide I (around 1,650 cm^{-1} and 1,550 cm^{-1}), and phosphate groups (around 1,020 cm^{-1}) were observed in each area.

Fig. 5 shows the results of imaging measurements of the contact surface between the adjacent vertebrae and the PEEK cage with the OCP/Gel implanted. As with Fig. 3, the imaging shows the relative distribution by mapping the absorption intensity ratio divided between the absorption intensities derived from amide I and phosphate groups. The area of accumulation of phosphate groups, which suggests OCP granules, is small, and the area of amide I, which suggests bone matrix-derived proteins, is larger than in Fig. 3.

The IR spectra extracted from the arrowed points (black, green, red, and yellow arrows) shown in the imag-

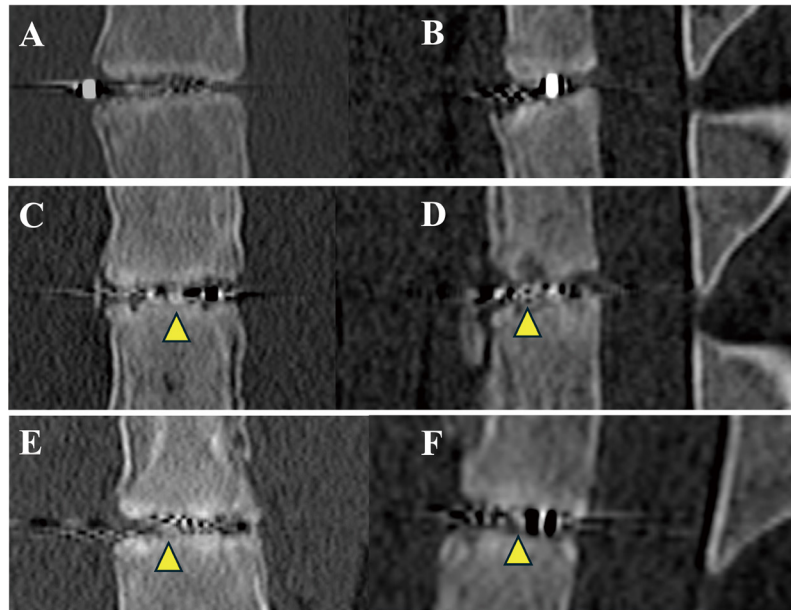


Fig. 1. Computed tomography images.

A, B: Coronal and sagittal images of lumbar Interbody fusion with PEEK cage. C, D: Coronal and sagittal images of lumbar Interbody fusion with PEEK cage and autologous rib. E, F: Coronal and sagittal images of lumbar Interbody fusion with PEEK cage and OCP/Gel. Eight weeks after surgery, partial bone fusion (indicated by yellow arrowheads) was observed following the implantation of autologous bone or the OCP/Gel composite in a PEEK cage for lumbar fusion. Gel, gelatin; OCP, octacalcium phosphate; PEEK, polyetheretherketone.

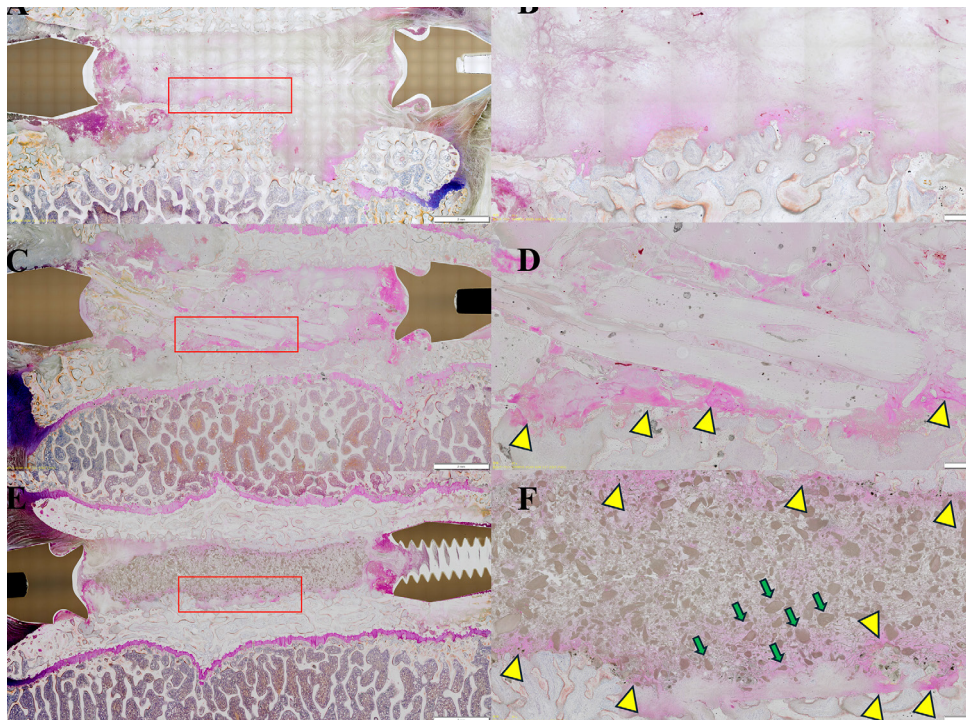


Fig. 2. Non-demineralized histological assessment.

A, B: Lower and higher magnification histological images of lumbar Interbody fusion with PEEK cage. C, D: Lower and higher magnification histological images of lumbar Interbody fusion with PEEK cage and autologous rib. E, F: Lower and higher magnification histological images of lumbar Interbody fusion with PEEK cage and OCP/Gel. Using a cage implanted with autologous bone or the OCP/Gel composite, new bone (indicated by yellow arrowheads) was observed forming at the interface between the PEEK cage and the vertebral body. Residual OCP (green arrows) showed varying degrees of biodegradation and appeared in different sizes. New bone formation was also confirmed around the OCP near the vertebral body interface. Scale bars indicate 2 mm in A, C, and E and 500 μ m in B, D, and F. Gel, gelatin; OCP, octacalcium phosphate; PEEK, polyetheretherketone.

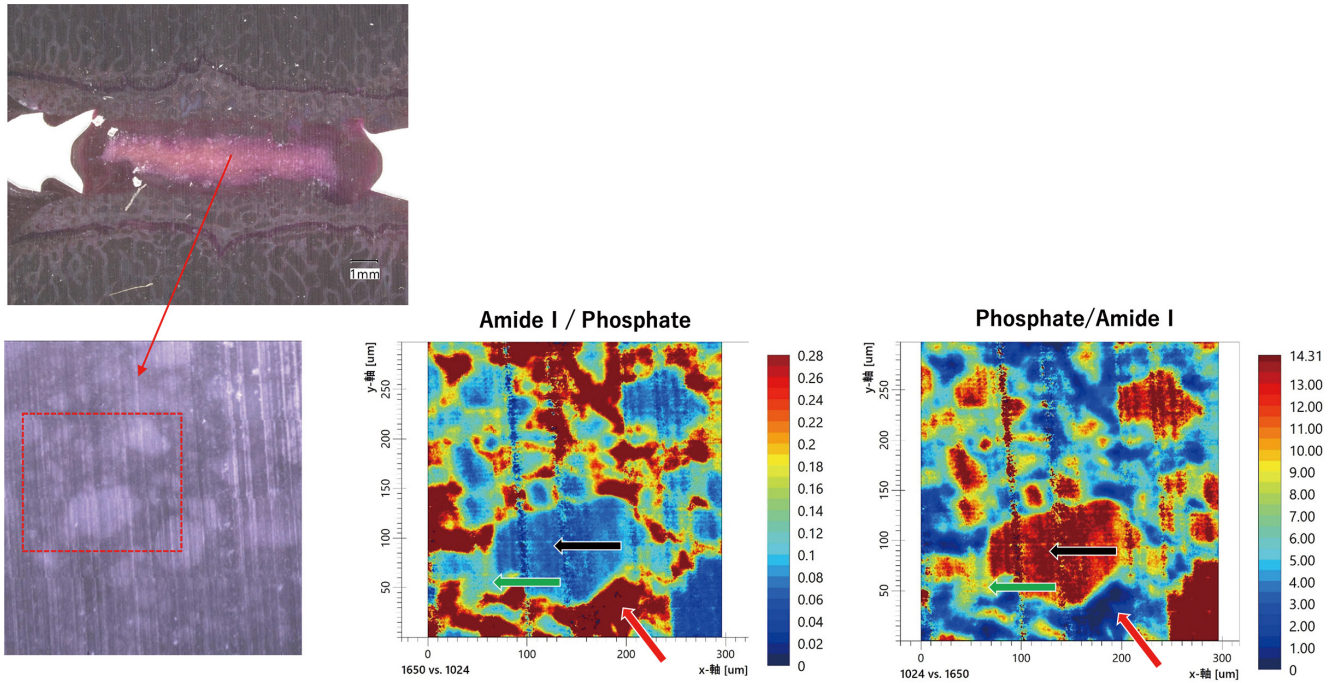


Fig. 3. FT-IR analysis of the inside of PEEK cage and OCP/Gel implantation site. The mapping of the ratio of amide I to phosphate and its reciprocal are shown. FT-IR, Fourier transform infrared; Gel, gelatin; OCP, octacalcium phosphate; PEEK, polyetheretherketone.

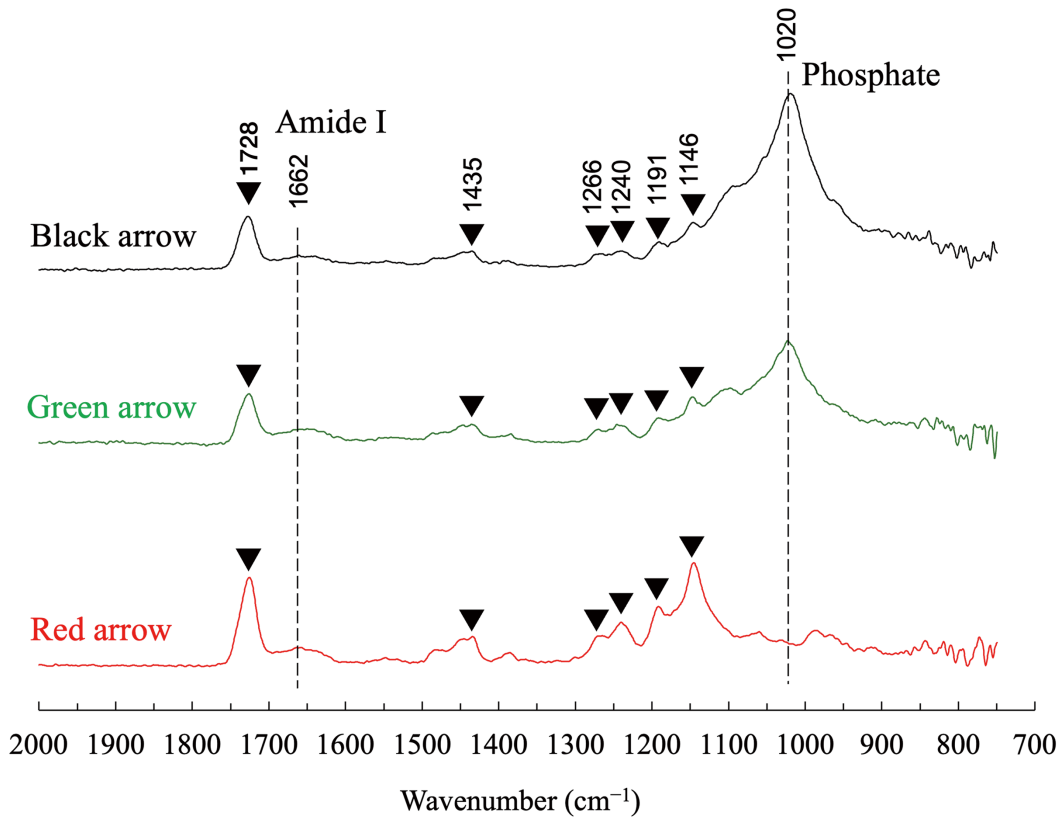


Fig. 4. IR spectra extracted from arbitrary locations inside of PEEK cage OCP/Gel filled. Each graph shows the spectra of the arrowed sites shown in Fig. 3. Peaks suggestive of amide I, phosphate, and acrylic embedding resin (black marks) are shown. IR, infrared; Gel, gelatin; OCP, octacalcium phosphate; PEEK, polyetheretherketone.

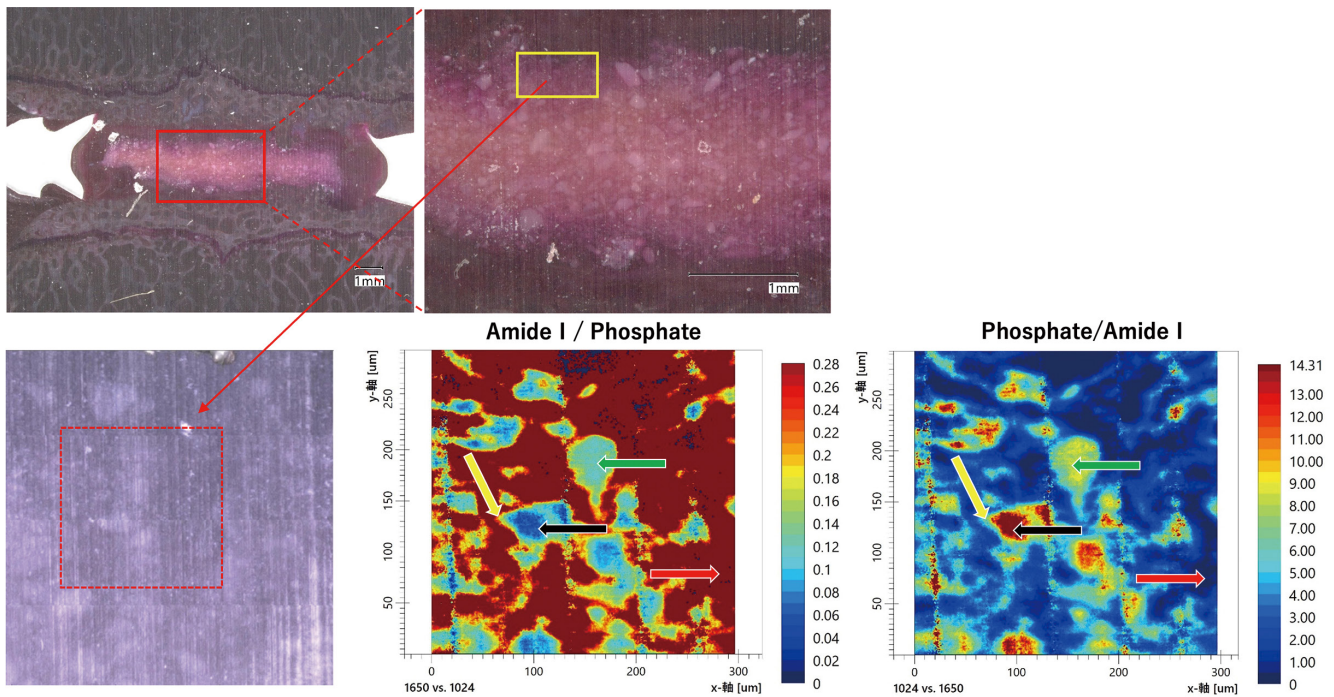


Fig. 5. FT-IR analysis of the surface area of PEEK cage and OCP/Gel implantation site.

The mapping of the ratio of amide I to phosphate and its reciprocal are shown. FT-IR, Fourier transform infrared; Gel, gelatin; OCP, octacalcium phosphate; PEEK, polyetheretherketone.

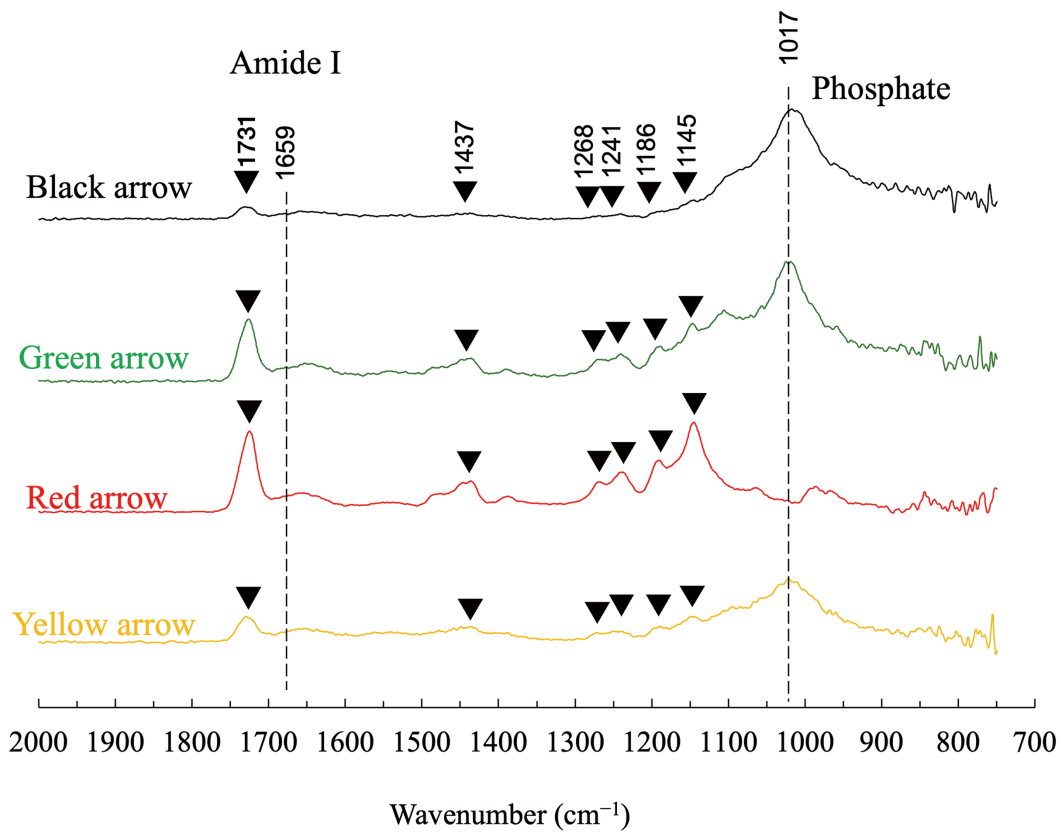


Fig. 6. IR spectra extracted from arbitrary locations in the surface area of PEEK cage OCP/Gel filled.

Each graph shows the spectra of the arrowed sites shown in Fig. 5. Peaks suggestive of amide I, phosphate, and acrylic embedding resin (black marks) are shown. IR, infrared; Gel, gelatin; OCP, octacalcium phosphate; PEEK, polyetheretherketone.

Table 1. Absorption intensity from arbitrary location within the PEEK cage OCP/Gel filled area.

Inside Cage			
	Absorption Intensity		Absorption Intensity Ratio
	Phosphate (1,020 cm^{-1})	Amide I (1,662 cm^{-1})	Phosphate (1,020 cm^{-1}) / Amide I (1,662 cm^{-1})
Black arrow	0.3426	0.0199	17.17
Green arrow	0.2002	0.0312	6.41
Red arrow	0.0268	0.0323	0.83
Surface area			
	Absorption Intensity		Absorption Intensity Ratio
	Phosphate (1,017 cm^{-1})	Amide I (1,659 cm^{-1})	Phosphate (1,017 cm^{-1}) / Amide I (1,659 cm^{-1})
Black arrow	0.2671	0.0133	20.05
Green arrow	0.2919	0.0408	7.14
Red arrow	0.0106	0.0436	0.24
Yellow arrow	0.1658	0.0261	6.34

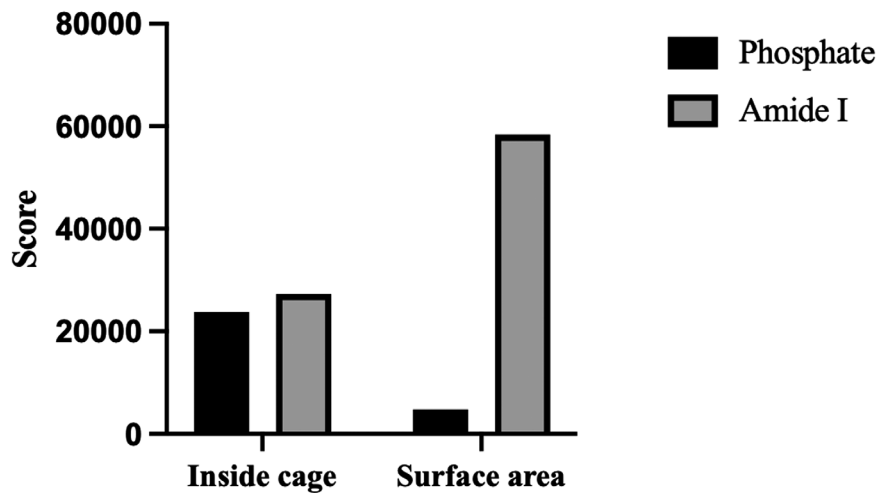


Fig. 7. Accumulated scores of amide I and phosphate ratio for OCP/Gel filled PEEK cage internal and surface regions.

In the mapping of amide I/phosphate groups in Figs. 3 and 5, the composite values after binarization within the imaging measurement area were compared for (1) an intensity ratio of less than 0.1, which is defined as a phosphate group and its value is “1”, and (2) an intensity ratio of 0.2 or greater, which is defined as an amide I group and its value is “1”, respectively.

ing measurement results in Fig. 5 are shown in Fig. 6. At each location, peaks mainly derived from acrylic embedding resin (marked in the Figure), amide I (around 1,650 cm^{-1} and 1,550 cm^{-1}), and phosphate groups (around 1,020 cm^{-1}) were observed.

Table 1 shows the quantitative values of the absorption intensities of the phosphate group (around 1,020 cm^{-1}) and amide I (around 1,650 cm^{-1}) for the arrowed parts of Figs. 3 and 5, and the ratio of the absorption intensities of the phosphate group (around 1,020 cm^{-1}) and amide I (around 1,650 cm^{-1}) for each.

Fig. 7 shows the results of the quantitative analysis of the proportions of phosphate and amide I within the imaging measurement area. Specifically, in the mapping of amide I/phosphate groups in Figs. 3 and 5, (1) when the intensity ratio is defined as less than 0.1 as the phosphate group and the value is set to “1”, (2) when the intensity

ratio is defined as 0.2 or more as the amide I group and the value is set to “1”, the combined values after binarization within the imaging measurement area were compared for each. Analysis of the inside of the cage with OCP/Gel implanted showed that there was a slightly higher level of amide I compared to phosphate. On the other hand, the formation of amide I was high near the contact surface between the cage and the vertebral body when using OCP/Gel, suggesting the presence of abundant bone matrix-derived proteins.

Discussion

In this study, computed tomography analysis and histological analysis of non-decalcified specimens confirmed that interbody fusion using a PEEK cage with OCP/Gel did not differ significantly from interbody fusion using a PEEK cage with autologous rib in terms of bone fusion. In addi-

tion, FT-IR analysis of OCP/Gel inside the PEEK cage placed in the disc space confirmed a decrease in phosphate groups due to degradation of OCP at the contact surface with the vertebral body and an increase in bone matrix proteins due to OCP-induced osteogenesis. In the analysis of OCP/Gel in the center of the PEEK cage, an increase in amide I reflecting bone matrix formation was observed, indicating that OCP/Gel may be effective not only for direct implantation in bone but also for implantation in the PEEK cage in the intervertebral disc space. When examining the results of the FT-IR spectrum, it is possible that the phosphate group band around $1,020\text{ cm}^{-1}$ also includes a contribution from bone apatite crystals derived from new bone. The authors interpreted the peak at this frequency as being due to phosphate groups derived from OCP, but by considering the formation of new bone at week 8, it can also be interpreted as including phosphate groups from bone apatite. Therefore, when considered together with the appearance of Amide I, it suggests that OCP is being broken down while promoting the formation of apatite. The induction of new bone tissue observed even in the center of the PEEK cage may be derived from the capability of orthotopic bone formation that OCP initiates new bone formation from its own surface even at a location far from the existing bone (Imaizumi et al. 2006; Kikawa et al. 2009) which is due to not only the accumulation of mesenchymal stem cells around the material surface but also the stimulatory capacity toward osteoblastic differentiation from mesenchymal stem cells (Okuyama et al. 2022).

Lumbar interbody fusion is commonly used to treat degenerative spinal diseases. The ideal bone graft material for interbody fusion requires osteoinductivity, osteoconductivity, and excellent mechanical properties. Ilium bone grafts have all the characteristics necessary for an ideal bone graft, such as trabecular structure as a bone conduction scaffold, osteoinductive bone morphogenetic proteins, and osteogenic cells, so they have been used for a long time (Banwart et al. 1995; Galimberti et al. 2015). However, due to the limited amount that can be harvested (Myeroff and Archdeacon 2011) and the serious complications associated with IBCG harvesting, there is a growing interest in finding alternative transplant materials (Banwart et al. 1995; Yoshii et al. 2021). Good clinical results have been reported for lumbar interbody fusion surgery using synthetic bone in which bone morphogenetic protein 2 is used in combination with HA/Col (Kushioka et al. 2018) or artificial bone in which bone marrow aspirate is used in combination with HA/Col, implanted in a cage (Yoshii et al. 2021). However, compared to autologous iliac bone grafting, the collection of bone marrow aspirate is minimally invasive, but ideally, equivalent results should be obtained with only high-performance synthetic bone graft substitutes. The results of this study indicate that OCP/Gel may be useful in cage-based interbody fusion surgery without the need for invasive bone marrow aspiration or expensive growth factors like bone morphogenetic protein 2.

On the basis of the promising results of the OCP/Gel combination (Hamada et al. 2022) and in view of its clinical application in dental reconstructive surgery (Kawai et al. 2020), a careful step-by-step approach to clinical trials should be taken. A small case series using autologous bone grafting as a control should be the first step in clinical trials. Another good place to start is with a small randomized controlled trial using the OCP/Gel composite in stable bone defects that occur after fracture treatment implant removal and curettage of benign bone lesions. The control group should include an autograft and/or another calcium phosphate substitute that is Japanese pharmaceuticals and medical devices agency-approved and has established clinical and radiologic results. After convincing results are observed in the first stage of clinical trials, subsequent clinical trials may be expanded to include larger defects, such as those associated with trauma or encountered during reconstructive surgery. Alternatively, they may become available for use in lumbar interbody fusion surgery.

Conclusion

The study explored the effectiveness of a PEEK cage combined with OCP/Gel for lumbar interbody fusion, comparing it to a PEEK cage with an autologous rib in a miniature swine interbody fusion model. Results from computed tomography and histological analyses showed no significant difference in interbody fusion between the two fillers. Further, FT-IR analysis revealed that the OCP/Gel inside the PEEK cage underwent phosphate group degradation at the interface with the vertebral body, and there was an increase in bone matrix proteins, suggesting OCP-induced osteogenesis. Additionally, an increase in amide I in the OCP/Gel at the center of the cage indicated bone matrix formation, supporting the potential of OCP/Gel for use not only in direct bone implantation but also within PEEK cages in the intervertebral disc space. Our research also suggests that OCP/Gel is an excellent synthetic bone graft substitute with clinical applications.

Author Contributions

Mori, Y., Hamai, R., and Suzuki, O. conceived the original idea. Mori, Y., Kanabuchi, R., Onoki, T., Takahashi, K., and Hashimoto, K. performed the animal experiment. Mori, Y., Hamai, R., Kanabuchi, R., and Suzuki, O. performed computed tomography analysis, histological analysis, and FT-IR analysis. Mori, Y., Hamai, R., Aizawa, T., and Suzuki, O. wrote the manuscript. All authors have read and approved the final submitted manuscript.

Funding

This study was funded by JSPS KAKENHI to Mori Y. (grant number 23K08604) and Suzuki O. (grant number 21H03121).

Conflict of Interest

The authors declare no conflict of interest.

References

- Anada, T., Kumagai, T., Honda, Y., Masuda, T., Kamijo, R., Kamakura, S., Yoshihara, N., Kuriyagawa, T., Shimauchi, H. & Suzuki, O. (2008) Dose-dependent osteogenic effect of octacalcium phosphate on mouse bone marrow stromal cells. *Tissue Eng. Part A*, **14**, 965-978.
- Baba, K., Shiwaku, Y., Hamai, R., Mori, Y., Anada, T., Tsuchiya, K., Oizumi, I., Miyatake, N., Itoi, E. & Suzuki, O. (2020) Chemical Stability-Sensitive Osteoconductive Performance of Octacalcium Phosphate Bone Substitute in an Ovariectomized Rat Tibia Defect. *ACS Appl. Bio Mater.*, **3**, 1444-1458.
- Banwart, J.C., Asher, M.A. & Hassanein, R.S. (1995) Iliac crest bone graft harvest donor site morbidity. A statistical evaluation. *Spine (Phila Pa 1976)*, **20**, 1055-1060.
- Bohner, M., Santoni, B.L.G. & Döbelin, N. (2020) beta-tricalcium phosphate for bone substitution: Synthesis and properties. *Acta Biomater.*, **113**, 23-41.
- Brown, W.E. (1966) Crystal growth of bone mineral. *Clin. Orthop. Relat. Res.*, **44**, 205-220.
- Chiba, S., Anada, T., Suzuki, K., Saito, K., Shiwaku, Y., Miyatake, N., Baba, K., Imaizumi, H., Hosaka, M., Itoi, E. & Suzuki, O. (2016) Effect of resorption rate and osteoconductivity of biodegradable calcium phosphate materials on the acquisition of natural bone strength in the repaired bone. *J. Biomed. Mater. Res. A*, **104**, 2833-2842.
- Ezoe, Y., Anada, T., Yamazaki, H., Handa, T., Kobayashi, K., Takahashi, T. & Suzuki, O. (2015) Characterization of partially hydrolyzed OCP crystals deposited in a gelatin matrix as a scaffold for bone tissue engineering. *J. Nanopart. Res.*, **17**, 127.
- Galimberti, F., Lubelski, D., Healy, A.T., Wang, T., Abdullah, K.G., Nowacki, A.S., Benzel, E.C. & Mroz, T.E. (2015) A Systematic Review of Lumbar Fusion Rates With and Without the Use of rhBMP-2. *Spine (Phila Pa 1976)*, **40**, 1132-1139.
- Giannoudis, P.V., Dinopoulos, H. & Tsiroidis, E. (2005) Bone substitutes: an update. *Injury*, **36** Suppl 3, S20-27.
- Grecula, M.J. (2022) CORR Insights(R): Octacalcium Phosphate/Gelatin Composite (OCP/Gel) Enhances Bone Repair in a Critical-sized Transcortical Femoral Defect Rat Model. *Clin. Orthop. Relat. Res.*, **480**, 2056-2058.
- Hamada, S., Mori, Y., Shiwaku, Y., Hamai, R., Tsuchiya, K., Baba, K., Oizumi, I., Kanabuchi, R., Miyatake, N., Aizawa, T. & Suzuki, O. (2022) Octacalcium Phosphate/Gelatin Composite (OCP/Gel) Enhances Bone Repair in a Critical-sized Transcortical Femoral Defect Rat Model. *Clin. Orthop. Relat. Res.*, **480**, 2043-2055.
- Hamai, R., Sakai, S., Shiwaku, Y., Anada, T., Tsuchiya, K., Ishimoto, T., Nakano, T. & Suzuki, O. (2022) Octacalcium phosphate crystals including a higher density dislocation improve its materials osteogenicity. *Applied Materials Today*, **26**, 101279.
- Handa, T., Anada, T., Honda, Y., Yamazaki, H., Kobayashi, K., Kanda, N., Kamakura, S., Echigo, S. & Suzuki, O. (2012) The effect of an octacalcium phosphate co-precipitated gelatin composite on the repair of critical-sized rat calvarial defects. *Acta Biomater.*, **8**, 1190-1200.
- Honda, Y., Kamakura, S., Sasaki, K. & Suzuki, O. (2007) Formation of bone-like apatite enhanced by hydrolysis of octacalcium phosphate crystals deposited in collagen matrix. *J. Biomed. Mater. Res. B Appl. Biomater.*, **80**, 281-289.
- Imaizumi, H., Sakurai, M., Kashimoto, O., Kikawa, T. & Suzuki, O. (2006) Comparative study on osteoconductivity by synthetic octacalcium phosphate and sintered hydroxyapatite in rabbit bone marrow. *Calcif. Tissue Int.*, **78**, 45-54.
- Ishiko-Uzuka, R., Anada, T., Kobayashi, K., Kawai, T., Tanuma, Y., Sasaki, K. & Suzuki, O. (2017) Oriented bone regenerative capacity of octacalcium phosphate/gelatin composites obtained through two-step crystal preparation method. *J. Biomed. Mater. Res. B Appl. Biomater.*, **105**, 1029-1039.
- Ito, K., Mori, Y., Kamimura, M., Koguchi, M., Kurishima, H., Koyama, T., Mori, N., Masahashi, N., Hanada, S., Itoi, E. & Aizawa, T. (2022) beta-type TiNbSn Alloy Plates With Low Young Modulus Accelerates Osteosynthesis in Rabbit Tibiae. *Clin. Orthop. Relat. Res.*, **480**, 1817-1832.
- Kawai, T., Kamakura, S., Matsui, K., Fukuda, M., Takano, H., Iino, M., Ishikawa, S., Kawana, H., Soma, T., Imamura, E., Kizu, H., Michibata, A., Asahina, I., Miura, K., Nakamura, N., et al. (2020) Clinical study of octacalcium phosphate and collagen composite in oral and maxillofacial surgery. *J. Tissue Eng.*, **11**, 2041731419896449.
- Kikawa, T., Kashimoto, O., Imaizumi, H., Kokubun, S. & Suzuki, O. (2009) Intramembranous bone tissue response to biodegradable octacalcium phosphate implant. *Acta Biomater.*, **5**, 1756-1766.
- Kikuchi, M., Itoh, S., Ichinose, S., Shinomiya, K. & Tanaka, J. (2001) Self-organization mechanism in a bone-like hydroxyapatite/collagen nanocomposite synthesized in vitro and its biological reaction in vivo. *Biomaterials*, **22**, 1705-1711.
- Koguchi, M., Mori, Y., Kamimura, M., Ito, K., Tanaka, H., Kurishima, H., Koyama, T., Mori, N., Masahashi, N. & Aizawa, T. (2023) Low Young's Modulus TiNbSn Alloy Locking Plates Accelerate Osteosynthesis in Rabbit Tibiae. *Tohoku J. Exp. Med.*, **261**, 199-209.
- Kogure, A., Mori, Y., Tanaka, H., Kamimura, M., Masahashi, N., Hanada, S. & Itoi, E. (2019) Effects of elastic intramedullary nails composed of low Young's modulus Ti-Nb-Sn alloy on healing of tibial osteotomies in rabbits. *J. Biomed. Mater. Res. B Appl. Biomater.*, **107**, 700-707.
- Kushioka, J., Kaito, T., Makino, T., Fujiwara, H., Tsukazaki, H., Takenaka, S., Sakai, Y. & Yoshikawa, H. (2018) Difference in the fusion rate and bone formation between artificial bone and iliac autograft inside an inter-body fusion cage - A comparison between porous hydroxyapatite/type 1 collagen composite and autologous iliac bone. *J. Orthop. Sci.*, **23**, 622-626.
- LeGeros, R.Z. (2002) Properties of osteoconductive biomaterials: calcium phosphates. *Clin. Orthop. Relat. Res.*, **395**, 81-98.
- Miyatake, N., Kishimoto, K.N., Anada, T., Imaizumi, H., Itoi, E. & Suzuki, O. (2009) Effect of partial hydrolysis of octacalcium phosphate on its osteoconductive characteristics. *Biomaterials*, **30**, 1005-1014.
- Mori, Y., Hamai, R., Aizawa, T. & Suzuki, O. (2023) Impact of Octacalcium Phosphate/Gelatin (OCP/Gel) Composite on Bone Repair in Refractory Bone Defects. *Tohoku J. Exp. Med.*, **260**, 245-252.
- Murakami, Y., Honda, Y., Anada, T., Shimauchi, H. & Suzuki, O. (2010) Comparative study on bone regeneration by synthetic octacalcium phosphate with various granule sizes. *Acta Biomater.*, **6**, 1542-1548.
- Myeroff, C. & Archdeacon, M. (2011) Autogenous bone graft: donor sites and techniques. *J. Bone Joint Surg. Am.*, **93**, 2227-2236.
- Ogose, A., Hotta, T., Kawashima, H., Kondo, N., Gu, W., Kamura, T. & Endo, N. (2005) Comparison of hydroxyapatite and beta tricalcium phosphate as bone substitutes after excision of bone tumors. *J. Biomed. Mater. Res. B Appl. Biomater.*, **72**, 94-101.
- Ogose, A., Kondo, N., Umezumi, H., Hotta, T., Kawashima, H., Tokunaga, K., Ito, T., Kudo, N., Hoshino, M., Gu, W. & Endo, N. (2006) Histological assessment in grafts of highly purified beta-tricalcium phosphate (OSferion) in human bones. *Biomaterials*, **27**, 1542-1549.
- Oizumi, I., Hamai, R., Shiwaku, Y., Mori, Y., Anada, T., Baba, K., Miyatake, N., Hamada, S., Tsuchiya, K., Nishimura, S.N., Itoi, E. & Suzuki, O. (2021) Impact of simultaneous hydrolysis of OCP and PLGA on bone induction of a PLGA-OCP composite scaffold in a rat femoral defect. *Acta Biomater.*, **124**, 358-373.
- Okuyama, K., Shiwaku, Y., Hamai, R., Mizoguchi, T., Tsuchiya, K., Takahashi, T. & Suzuki, O. (2022) Differentiation of

- committed osteoblast progenitors by octacalcium phosphate compared to calcium-deficient hydroxyapatite in Lepr-cre/Tomato mouse tibia. *Acta Biomater.*, **142**, 332-344.
- Sato, T., Anada, T., Hamai, R., Shiwaku, Y., Tsuchiya, K., Sakai, S., Baba, K., Sasaki, K. & Suzuki, O. (2019) Culture of hybrid spheroids composed of calcium phosphate materials and mesenchymal stem cells on an oxygen-permeable culture device to predict in vivo bone forming capability. *Acta Biomater.*, **88**, 477-490.
- Sotome, S., Ae, K., Okawa, A., Ishizuki, M., Morioka, H., Matsumoto, S., Nakamura, T., Abe, S., Beppu, Y. & Shinomiya, K. (2016) Efficacy and safety of porous hydroxyapatite/type I collagen composite implantation for bone regeneration: A randomized controlled study. *J. Orthop. Sci.*, **21**, 373-380.
- Suzuki, O., Kamakura, S., Katagiri, T., Nakamura, M., Zhao, B., Honda, Y. & Kamijo, R. (2006) Bone formation enhanced by implanted octacalcium phosphate involving conversion into Ca-deficient hydroxyapatite. *Biomaterials*, **27**, 2671-2681.
- Suzuki, O., Nakamura, M., Miyasaka, Y., Kagayama, M. & Sakurai, M. (1991) Bone formation on synthetic precursors of hydroxyapatite. *Tohoku J. Exp. Med.*, **164**, 37-50.
- Takami, M., Mochizuki, A., Yamada, A., Tachi, K., Zhao, B., Miyamoto, Y., Anada, T., Honda, Y., Inoue, T., Nakamura, M., Suzuki, O. & Kamijo, R. (2009) Osteoclast differentiation induced by synthetic octacalcium phosphate through receptor activator of NF-kappaB ligand expression in osteoblasts. *Tissue Eng. Part A*, **15**, 3991-4000.
- Tamai, N., Myoui, A., Tomita, T., Nakase, T., Tanaka, J., Ochi, T. & Yoshikawa, H. (2002) Novel hydroxyapatite ceramics with an interconnective porous structure exhibit superior osteoconduction in vivo. *J. Biomed. Mater. Res.*, **59**, 110-117.
- Tanaka, H., Mori, Y., Noro, A., Kogure, A., Kamimura, M., Yamada, N., Hanada, S., Masahashi, N. & Itoi, E. (2016) Apatite Formation and Biocompatibility of a Low Young's Modulus Ti-Nb-Sn Alloy Treated with Anodic Oxidation and Hot Water. *PLoS One*, **11**, e0150081.
- Yamada, M., Anada, T., Masuda, T., Takano-Yamamoto, T. & Suzuki, O. (2015) Effect of mechanical stress on differentiation of mouse mesenchymal stem cells seeded into an octacalcium phosphate-gelatin scaffold. *Sensors and Actuators B: Chemical*, **220**, 125-130.
- Yoshii, T., Hashimoto, M., Egawa, S., Hirai, T., Inose, H. & Okawa, A. (2021) Hydroxyapatite/collagen composite graft for posterior lumbar interbody fusion: a comparison with local bone graft. *J. Orthop. Surg. Res.*, **16**, 639.
-